Mutations in the P-type cation-transporter ATPase 4, PfATP4, mediate resistance to both aminopyrazole and spiroindolone antimalarials

Erika L. Flannery[1], Case W. McNamara[2], Sang Wan Kim[1], Tomoyo Sakata Kato[2], Fengwu Li[3], Christine H. Teng[1], Kerstin Gagaring[2], Micah J. Manary[1], Rachel Barboa[2], Stephan Meister[1], Kelli Kuhen[2], Joseph M. Vinetz[3], Arnab K. Chatterjee[2], Elizabeth A. Winzeler[1]

Supporting Information

Materials and Methods

Evolution of compound-resistant parasites. The clonal *P. falciparum* multidrug resistant strain $Dd2^{EF1}$ was cultured in human red blood cells in RPMI 1640 media supplemented with 0.5% Albumax II, 4.3% human serum, 25 mM Hepes, 25 mM $NaHCO_3$, 0.36 mM hypoxanthine and 100 ug/mL gentamicin. Fresh blood was depleted of white cells using a Sepacell leukocyte reduction filter (Fenwal, Lake Zurich, IL). Cultures were incubated at 37°C in an atmosphere of 3% O_2, 4% CO_2 and 93% N_2. GNF-Pf4492 resistant parasites were selected for as described previously[1]. Briefly, three independent cultures of *P. falciparum* $Dd2^{EF1}$ were maintained in parallel at 2.5% hematocrit in the presence of increasing concentrations of GNF-Pf4492 over time. Resistance selection began at 200 nM, approximately the IC_{50} of GNF-Pf4492 against $Dd2^{EF1}$. Once parasites achieved parasitemias of 6-8%, parasites were diluted to 1% parasitemia and compound concentration was increased again, generally by 10%. GNF-Pf4492 was stored in 100% DMSO and added to cultures such that the DMSO concentration in culture never exceeded 0.1%. After ~70 days of selection, parasites were cloned in 96-well plates by limiting dilution[2]. Parasite resistance was stable and did not require continuous compound selection.

***In vitro* compound sensitivity assays.** The half maximal (50%) inhibitory concentration (IC_{50}) of each compound was determined in dose-response format using a SYBR Green I-based cell proliferation assay [3]. Parasites were incubated in 384 or 96-well format with exposure to a 20 or 12-point dilution series of compound. Following incubation for 72 hours (hr), parasites were lysed, DNA was stained using SYBR Green I and fluorescence was measured at 535 nm on an Envision plate reader (Perkin Elmer, Waltham, MA) after excitation at 485 nm. Four parameter dose-response curves were fit and $\log(IC_{50})$ values calculated using Prism (Graphpad Prism, La Jolla, CA).

Whole genome sequencing (WGS). DNA libraries of each sample were prepared using the Illumina TruSeq v. 3 protocol (Illumina, Inc., San Diego, CA) of fragmentation, end-repair and adapter ligation. Libraries were clustered and run on an Illumina HiSeq 2000 according to manufacturer's instructions. We obtained 50 base pair, single-end reads and analyzed raw data using CASAVA v. 1.8+. Sequences were aligned to the *P. falciparum* 3D7 reference genome (PlasmoDB v. 9.0) using the Burrows-Wheeler Aligner (BWA v.0.6.2) and then converted to an alignment map format using the Sequence Alignment/Map toolbox (SAMTools v.0.2.6). Sequence alignments were put through a custom quality control procedure that has been developed in our lab utilizing the Picard sequence toolbox (Picard v1.7.3)[4]. SNVs were initially detected using the Genome Analysis Toolkit (GATK v1.6) and then filtered using the Plasmodium Type Uncovering Software, an integrated pipeline developed in our lab that can also call CNVs [4].

Sanger sequencing. To confirm all non-synonymous SNVs identified in open-reading frames by WGS, genomic DNA was PCR amplified in 50 µL reaction volume with 2.5 µM dNTPs, and 1.0 unit Phusion polymerase (New England BioLabs, Ipswich, MA) using primers previously reported [1]. PCR products were sequenced directly (Eton Bioscience Inc, San Diego, CA).

Vector Construction, Protein Expression and Purification of PfATP4's N-domain

Amino acid alignment and homology modeling identified PfATP4 residues Ser450 and Arg754 as the likely borders of the nucleotide-binding domain (N-domain). The high solvent accessibility across the domain's surface, conserved fold and small molecular mass of this domain made it an ideal candidate for heterologous expression in *E. coli*. The N-domain was amplified by Phusion polymerase (Finnzymes) with the primers TATGCTAGCTCTGATAAAACCGGTACATTAACTG (NheI site underlined) and TATCTCGAG**TTA**TCTTGGGGGATCAAATGA (XhoI site underlined, stop codon in bold) using the subcloned *pfatp4* gene from the parental Dd2 genome as template. The PCR amplicon was digested with NheI and XhoI, then ligated into the respective restriction endonuclease sites of pET28b(+) yielding a construct with an N-terminal hexahistidine tag followed by a thrombin cleavage site. A positive clone was verified by Sanger sequencing and subsequently transformed into competent BL21-CodonPlus(DE3)-RIL cells (Stratagene).

Terrific Broth media (Sigma) was inoculated with a 1:100 dilution from a starter culture grown overnight and growth was continued at 37°C on a shaking platform. The optical density (OD) was monitored at 600 nm until the culture reached 0.7–0.8 OD_{600} at which time the incubation temperature was reduced to 20°C and isopropyl-ß-D-thiogalactoside (IPTG; Anatrace, USA) was added to a final concentration of 0.1 mM in the media to induce expression of the PfATP4 N-domain fragment. The cells were harvested after 14–16 h and the cell pellets were stored at -80°C until purification.

A two-step purification was executed to yield protein purity >90%. In brief, cells were disrupted by a combination of lysozyme and sonication, and clarified by centrifugation. The supernatant was incubated with Talon affinity resin (Clontech, USA) to capture the hexahistidine-tagged product. An on-column digestion with biotinylated thrombin (Novagen, USA) liberated the N-domain and fractions of highly purified protein were collected. The pooled eluant was incubated with streptavidin-immobilized resin (Novagen, USA) to remove the biotinylated thrombin and the column flow-through was dialyzed against PBS and 0.01% Tween 20. The protein was stored as frozen aliquots at 1 mg/mL. The protein concentration was determined by a detergent-compatible Bradford assay kit (BioRad, USA) and protein purity was confirmed by SDS-PAGE.

Antibody Production

The immunization of mice and titer determination by ELISA was performed as previously described [5]. Briefly, the RIMMS immunization protocol [6] was carried out using C57BL/6-Tg(BCL2)22Wehi/J mice. Two mice were immunized for 8 rounds with 50 µL 500 µg/mL purified PfATP4 N-domain per injection. Mouse serum was evaluated by ELISA for PfATP4 antibodies. Serum positive animals were sacrificed and pooled peripheral lymph nodes (PLN) were harvested.

Western blot analysis

In vitro cultured *P. falciparum* parasite lines (10 mL culture volume, 5–8% parasitemia, 2.5% hematocrit) were extracted with saponin to isolate parasites. The resultant parasite pellets were then lysed in 100 µL volume of PBS supplemented with 1% ASB 14-4 (Sigma) and a cOmplete, Mini, EDTA-free Protease Inhibitor Cocktail tablet (Roche). The lysate was clarified by a 5 min centrifugation step at 16,000×*g*, the resultant supernatant transferred to a fresh vial, and the samples stored at -80°C. Protein concentration of each supernatant was quantified using a detergent-compatible Bradford kit (Bradford*Ultra*; Expedeon). Lysates (10 or 50 µg total protein/well) were resolved by SDS-PAGE on a 4–20% tris-glycine gel and then transferred to a nitrocellulose membrane using the iBlot system (Life Technologies) for analysis by Western blot. Nonfat dry milk (Carnation) resuspended to 5%(w/v) in tris-buffered saline (50 mM tris, pH 7.6, 150 NaCl) with 0.05% (v/v)Tween 20 was used as the membrane blocking buffer. The custom polyclonal, mouse antisera raised against the N-domain of PfATP4 was diluted to 1:1,000 and the secondary antibody (sheep anti-mouse goat IgG conjugated to horseradish peroxidase (GE Healthcare)) was diluted to 1:2,500. Both antibodies were diluted into a modified blocking buffer with nonfat dry milk reduced to 1%. A SuperSignal West Femto Maximum Sensitivity Chemiluminescent Substrate kit (Pierce) was used to visualize the secondary antibodies using a ChemiDoc MP (Bio-Rad) Imaging System. Relative quantification of the PfATP4 bands (located between the 100 and 150 kDa SDS-PAGE standards) were measured using Image Lab (version 4.0.1).

PfATP4 homology modeling. A previously generated homology model of PfATP4 [1] was used to map the resistance-conferring mutations identified in the GNF-Pf4492-resistant lines. The PyMOL Molecular Graphics System (version 1.2r2, Schrödinger, LLC, Portland, OR) was used to render the model and prepare the figure.

Compound time of action. Highly synchronous cultures were achieved using the sorbitol synchronization method [7]. Double synchronized erythrocytic ring stage parasites were treated with drug and monitored over a 60 hr period. The morphology of parasites was recorded. Representative images are shown for each time point.

Protein synthesis inhibition studies. Metabolic labeling with [^{35}S]-methionine/cysteine was done as previously described [1]. Briefly, parasites were harvested from asynchronous

cultures and washed in methionine- and cysteine-free culturing media. [^{35}S]-Met/Cys incorporation was measured after 1 hr incubation with inhibitors. Parasites were extracted for radiographic measurement and average incorporation was expressed as a percent of that incorporated when no inhibitor was present.

Liver schizont assay. A previously described in vitro high-content imaging assay [8] was used to measure *P. yoelii* sporozoite proliferation in a transgenic hepatoma line (HepG2-A16-CD81-EGFP; obtained from the laboratory of Dominique Mazier (INSERM, France)). Sporozoites were freshly purified from malaria-infected *Anopheles stephensi* mosquitoes (14 days post blood meal) provided by the New York University Insectary Core Facility (New York, NY). Sporozoites and nuclei were visualized with a PyHSP70 antibody and Hoechst stain, respectively, and the mean parasite area was quantified with an Opera Confocal High Content Screening System (PerkinElmer, Waltham, MA). Atovaquone and DMSO-treated wells were used as controls and IC_{50} values were determined by applying a standard logistic regression model.

Standard membrane feeding assay. *P. falciparum* NF54 was maintained in vitro in continuous cultivation with daily media changes and without the addition of fresh red blood cells to stimulate gametocytogenesis. Day 13, 15 and 17 gametocyte cultures that exhibited exflagellation were combined and centrifuged to form a 50 μL pellet. Mosquitoes were fed on a fresh blood meal (total volume = 200 μL) formulated to 50% hematocrit, with 25% human serum, with the 50 μL gametocyte pellet supplemented with GNF-Pf4492 or KAF246 at 1×, 10× or 100× the mean IC_{50} value for blood-stage parasites. Five to seven day old female *A. stephensi* mosquitoes were fed for 20 min using artificial membrane feeders. Twenty to forty mosquitoes were used for each feeding and control and compound-treated feeds were performed on the same day. Engorged mosquitoes were maintained with 10% glucose at 26°C and 80% relative humidity. Eight days post-feeding mosquito midguts were dissected and stained with 0.1% mercurochrome to enumerate the number of oocysts present by microscopy.

Determination of intracellular [Na^+]. Intracellular sodium concentration ($[Na^+]_i$) within the parasite was determined using the sodium-sensitive dye SBFI (Molecular Probes, Eugene, OR) as previously described[9] with the following modifications. Parasites were loaded at 1×10^9 cells/mL with 5.5 μM SBFI and 0.01% (w/v) Pluronic-F127 solution. The cell suspension was incubated at 37°C for 1 hr in the dark. Cells were then washed twice with BCF-RPMI and incubated for another 20 min at 37°C in the dark to allow for de-esterification of the dye. 50 μL of dye-loaded cells (2×10^9 cells/mL) were seeded into a black 384-well assay plate (Greiner Bio-One, Monroe, NC) and fluorescence was measured on an EnVision® Multilabel reader (PerkinElmer, Waltham, MA). Emission fluorescence was acquired at 490 nm after excitation at both 340 nm and 380 nm and real-time traces are reported for the ratio of the intensities. Compound or saline was added immediately prior to fluorescence acquisition. $[Na^+]_i$ was determined with the

equation $[Na^+]_i = b\{(R_n - R_{n(min)})/[a + R_{n(min)}) - R_n]\}$ where R_n is the fluorescence ratio normalized to $[Na^+]_i$ = 20 mM. The constants a, b, and $R_{n(min)}$ were determined by fitting a hyperbolic 3-point calibration curve to the following equation: $R_n = R_{n(min)} + [a([Na^+]_i)/(b + [Na+]_i)]$[10]. Calibration curves were performed for each strain and each day of measurement.

Figure Legends

Figure *S*1. *In vitro* evolution of GNF-Pf4492-R lines. Three independent lines of clonal *P. falciparum* $Dd2^{EF1}$ were cultured in the presence of increasing, sub-lethal GNF-Pf4492 concentrations, over time, beginning with approximately the IC_{50} for GNF-Pf4492 (200 nM). Cultures remained at this concentration for approximately 10 days, but appeared very unhealthy. Compound selection was removed for 3 days and then supplemented with 150nM GNF-Pf4492. Parasites grew better at this concentration and eventually compound concentration was increased when parasitemias reached 6-8% and the culture appeared healthy by cell morphology. The concentration of compound was generally increased by 10% at each step, but depended on factors such as parasite morphology, length of exposure at previous compound concentration and parasitemia.

Figure *S*2. Analysis of change in read count to detect CNVs. (*A*) Aligned sequencing read count in GNF-Pf4492R-1 compared to the *P. falciparum* 3D7 reference. The 14 *P. falciparum* chromosomes are represented. Differences in copy number detected by the CNV calling algorithm are identified when the bold black line drops above or below where the y-axis corresponds to a copy number of 1. The CNVs on chromosomes 5 and 12 are detected (red ellipse). (*B*) Aligned sequencing read count in GNF-Pf4492R-1 compared to the $Dd2^{EF1}$ parent. CNVs on chromosomes 5 and 12 are no longer detected, because these CNVs occur in both lines. No additional CNVs are detected.

Figure *S*3. Whole genome sequencing SNV calls. *(A)* Whole genome sequencing read alignment at position 1,031,006 on chromosome 13 shows the alternate G called in some reads, while in other reads the reference A is called and an insertion is denoted (red ellipse). The multiple adenosine homopolymer tract causes a mis-alignment in the GNF-Pf4492R-1 line (top) resulting in a false-positive SNV call. The reference sequence was verified in the GNF-Pf4492R-1 line using Sanger Sequencing. *(B)* Single nucleotide variant identified in *pfcdpk5* (PF3D7_1338700). Alignment of sequencing reads shows the base pair change compared to the *P. falciparum* 3D7 reference sequence from A to C at position 1,528,577 on chromosome 13 (blue boxes) resulting in the K544N amino acid change. This mutation is present in all three resistant lines as well as the $Dd2^{EF1}$ parent.

Figure *S*4. **Protein expression levels of PfATP4 characterized by western blot.** (*A*) Western blot of parasite whole cell lysate (10 μg) for the PfATP4 transgenic lines hybridized with anti-PfATP4 antibody. (*B*) Western blot of whole cell lysate (50 μg) for the GNF-Pf4492-resistant lines hybridized with anti-PfATP4 antibody.

Figure *S*5. Protein synthesis activity in the presence of inhibitor. Unsynchronized Dd2 (*A*) or KAE609R-1 (*B*) parasites were treated for 1 hour with compound over a five-log dose range to determine the effect of inhibitor on radio-labelled methionine and cysteine incorporation. Radioactive counts were normalized to untreated cells and each

data point was plotted as the mean of two experiments performed in triplicate. Error bars represent standard deviation.

Figures S6. Effect of inhibitors on intracellular sodium levels. Effects of (*A*) aminopyrazole and (*B*) spiroindolone inhibitors on intracellular sodium concentration $[Na^+]_i$ in the GNF-Pf4492R-2 and -3 lines. $[Na^+]_i$ traces for extracted trophozoite-stage parasites treated with saline or inhibitor immediately prior to fluorescence acquisition. Inhibitors were added at 1×, 3× 10× or 100× the IC_{50} for the $Dd2^{EF1}$ parent. Traces are representative of those obtained from a minimum of four independent experiments performed in duplicate. (*C*) Three point hyperbolic calibration curves were fit for each strain for each cell preparation measured. Calibration curves that correspond to the traces depicted in (*A*) and (*B*) are shown.

FIGURES.

Figure S1.

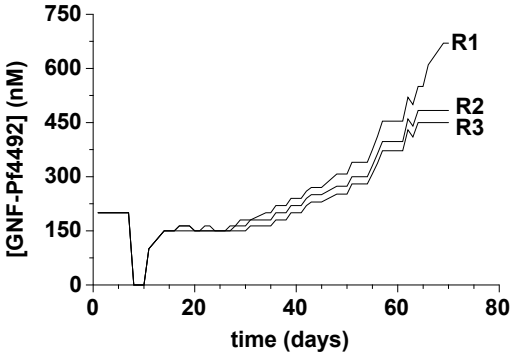

Figure S2.

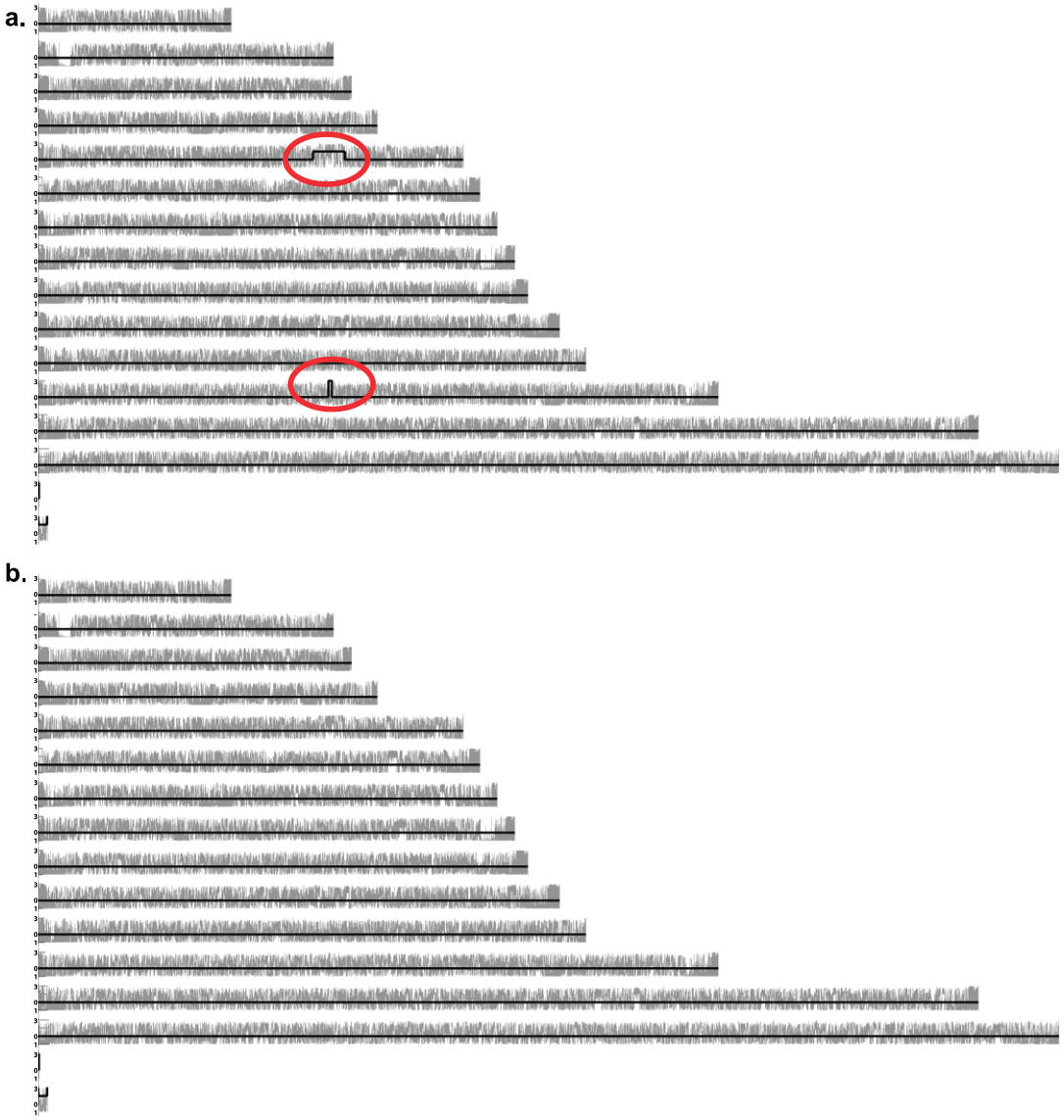

Figure S3.

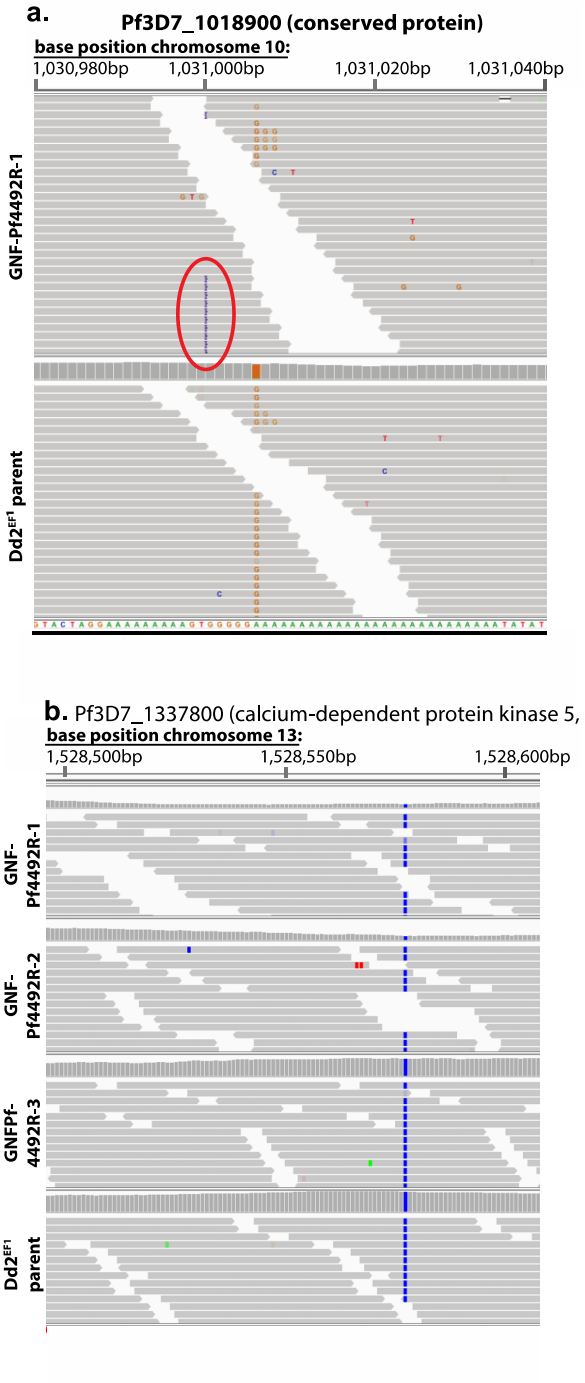
a.
Pf3D7_1018900 (conserved protein)
base position chromosome 10:
1,030,980bp
1,031,000bp
1,031,020bp
1,031,040bp
GNF-Pf4492R-1
Dd2EF1 parent
b. Pf3D7_1337800 (calcium-dependent protein kinase 5, CDPK5)
base position chromosome 13:
1,528,500bp
1,528,550bp
1,528,600bp
GNF-Pf4492R-1
GNF-Pf4492R-2
GNFPf-4492R-3
Dd2EF1 parent

Figure S4.

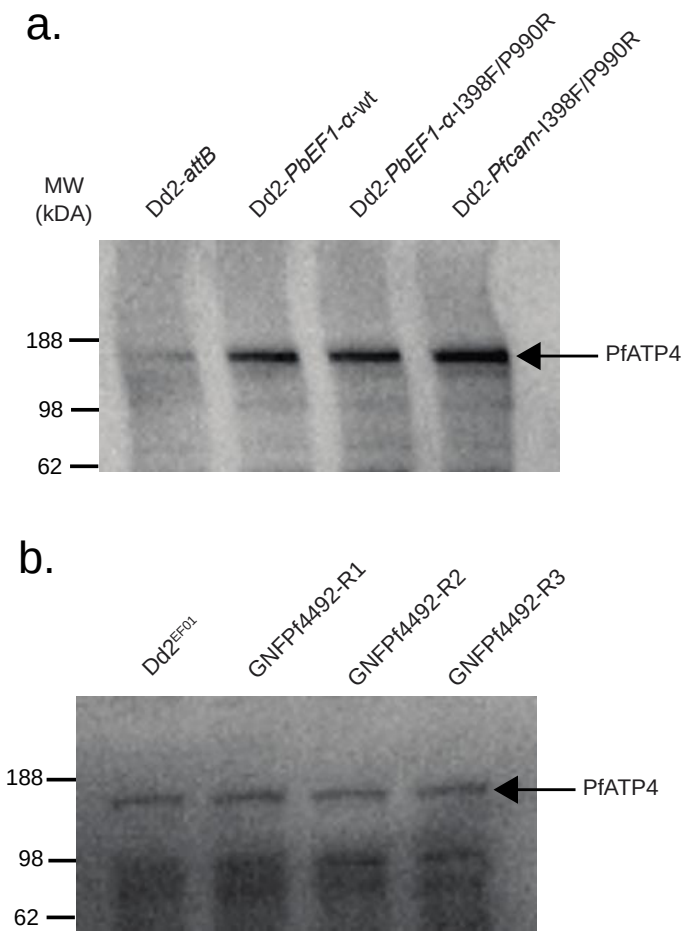
a.
MW
(kDA)
Dd2-attB
Dd2-PbEF1-α-wt
Dd2-PbEF1-α-I398F/P990R
Dd2-Pfcam-I398F/P990R
188
98
62
PfATP4
b.
Dd2EF01
GNFPf4492-R1
GNFPf4492-R2
GNFPf4492-R3
188
98
62
PfATP4

Figure S5.

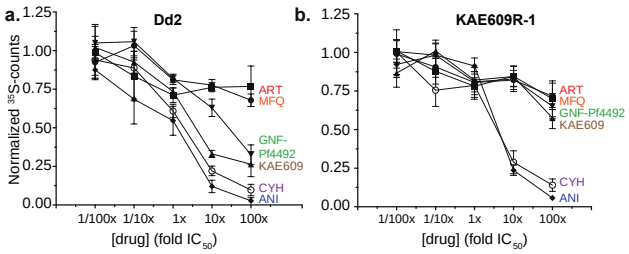
a.
Dd2
Normalized ^{35}S-counts
1.25
1.00
0.75
0.50
0.25
0.00
1/100x
1/10x
1x
10x
100x
[drug] (fold IC$_{50}$)
ART
MFQ
GNF-Pf4492
KAE609
CYH
ANI
b.
KAE609R-1
1.25
1.00
0.75
0.50
0.25
0.00
1/100x
1/10x
1x
10x
100x
[drug] (fold IC$_{50}$)
ART
MFQ
GNF-Pf4492
KAE609
CYH
ANI

Figure S6.

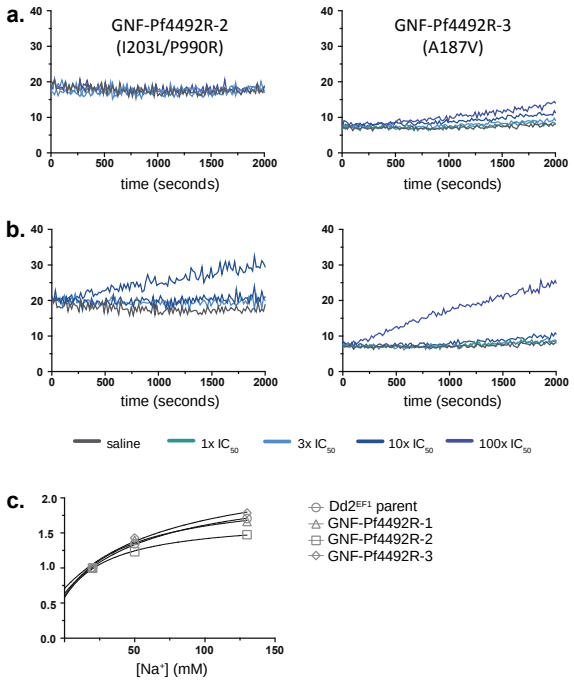
a.
GNF-Pf4492R-2
(I203L/P990R)
GNF-Pf4492R-3
(A187V)
time (seconds)
time (seconds)
b.
time (seconds)
time (seconds)
saline
1x IC50
3x IC50
10x IC50
100x IC50
c.
Dd2EF1 parent
GNF-Pf4492R-1
GNF-Pf4492R-2
GNF-Pf4492R-3
[Na+] (mM)

TABLES

Table S1. In vitro activity of select antimalarials against *P. falciparum* Dd2 lines.

	Fitted mean IC_{50} (95% CI (nM))[a]					
Aminopyrazole evolved resistant lines						
	ART	MFQ	GNF-Pf4492	KAF246	KAE678	KAE609
Dd2^{EF1}	20.9 (15.1-29.1)	14.6 (10.- 20.7)	184.1 (141.3-239.9)	0.428 (0.322-0.569)	27.5 (20.6-36.8)	0.690 (0.449-1.06)
GNF-Pf4492R-1	18.2 (12.5-26.6)	13.5 (8.74-20.8)	1170 (920.5-1483)[a]	0.0473 (0.0324-0.0693)[b]	1.63 (1.13-2.34)[b]	0.0615 (0.0564-0.0671)[b]
GNF-Pf4492R-2	18.1 (12.7-25.8)	11.3 (8.39-15.1)	811.0 (631.0-1040)[a]	3.02 (2.26-4.02)[b]	149 (70.3-316)[b]	2.85 (2.54-3.19)[b]
GNF-Pf4492R-3	18.5 (13.1-26.1)	16.1 (12.7-20.3)	631.0 (458.1-867.0)[a]	2.88 (2.20-3.77)[b]	140 (94.62-206)[b]	2.39 (1.44-3.98)[b]
Transgenic expression lines						
	ART	CQ	GNF-Pf4492	KAF246	KAE678	KAE609
Dd2^{attB}	15.5 (11.3, 21.2)	9.98 (2.27, 43.9)	203.7 (80.35, 515.2)	0.400 (0.172, 0.932)	ND	ND
Pb*ef1α*-wt	12.8 (3.62, 45.3)	9.12 (2.68, 31.0)	317.0 (135.8, 737.9)	0.574 (0.330, 1.00)	ND	ND
Pb*ef1α*-I398F/P990R	11.1 2.77, 44.7)	8.9 (3.15, 25.2)	396.3 (156.0, 1009)	0.837 (0.287, 2.44)	ND	ND
Pf*cam*-I398F/P990R	10.6 (1.63, 68.9)	9.06 (2.04, 40.3)	690.2 (437.5, 1086)[d]	1.96 (0.657, 5.83)[d]	ND	ND
Spiroindolone evolved resistant lines						
	ART	CQ	GNF-Pf4492	KAF246	KAE678	KAE609
Dd2^{CM1}	20.9 (19.1-22.8)	10.6 (7.83-14.3)	151 (133, 171)[b]	ND	31.8 (28.1, 36.0)[b]	0.671 (0.608, 0.743)[b]
KAE609R-1	17.5 (14.9-20.7)	12.3 (10.5-14.1)	1070 (786, 1450)[b]	ND	328 (289, 372)[b]	25.4 (3.60, 179)[b]
KAE609R-2	19.6 (16.0-24.0)	13.0 (10.6-16.0)	613 (496, 760)[b]	ND	236 (202, 275)[b]	5.47 (4.39, 6.84)[b]

KAE609R-3	10.3 (2.02-52.6)	13.0 (11.8-16.0)	458 (411, 511)[b]	ND	119 (113, 126)[b]	4.12 3.21, 5.30)[b]
KAE678R-1	19.8 (16.8-23.2)	12.4 (10.1-15.2)	1410 (1270, 1570)[b]	ND	247 (219, 279)[b]	4.14 (3.76, 4.56)[b]
KAE678R-2	33.4 (4.93-227)	11.9 (9.4, 15.1)	568 (507, 635)[b]	ND	227 (201, 249)[b]	3.66 (3.01, 4.45)[c]
KAE678R-3	18.1 (16.7-19.6)	12.4 (10.4, 14.8)	1600 (1410, 1800)[b]	ND	291 (275, 308)[b]	11.0 (1.93, 62.5)[b]

[a]Data are from a minimum of three experiments performed in duplicate using the SYBR green assay with a 72 hour incubation time. [b]$p<0.0001$; [c]$p<0.001$; and [d]$p<0.01$ after one-way ANOVA and Dunnett's multiple comparison posttest of the mean log(IC_{50}) values for each strain compared to the Dd2 parent. ND, not determined; ART, artemisinin; MFQ, mefloquine.

Table S2. Unique SNVs identified in GNF-Pf4492-resistant lines

Chr	Base position	Gene annotation	Mutation type (base change)	Reads[a]
		GNF-Pf4492R-1		
1	234556		Intergenic	33
4	216668		Intergenic	10
4	912762		Intergenic	15
5	134441		Intergenic	16
5	799254		Intergenic	22
5	1096964		Intergenic	20
5	1192574		Intergenic	25
6	545594		Intergenic	18
6	689064		Intergenic	21
6	1271683		Intergenic	9
8	385626	MAL8P1.300 (conserved protein)	Intron	13
8	458876		Intergenic	14
8	632603		Intergenic	35
8	754504	MAL8P1.80 (conserved protein)	Intron	23
8	1222811		Intergenic	13
9	692157	PFI0810c (apicoplast Ufd1 precursor)	Intron	23
9	1404327		Intergenic	32
10	753984	PF_0182 (conserved protein)	Nonsynonymous coding (aaA/aaT)	22
11	354437		Intergenic	13
11	965835		Intergenic	41
11	1162710		Intergenic	26
12	217106		Intergenic	26
12	532169	PFL0590c (PfATP4)	Nonsynonymous coding (Gca/Aca)	92
12	2007366		Intergenic	28
13	1031006	PF13_0139 (conserved protein)	Nonsynonymous coding (gAa/gGa)	54
13	1896826		Intergenic	26
13	2286117		Intergenic	26
13	2427955	MAL13P1.302 (SUMO ligase)	Intron	32

GNF-Pf4492R-2				
1	234556		Intergenic	23
4	244312		Intergenic	3
4	998202		Intergenic	12
5	674955		Intergenic	16
5	858856		Intergenic	15
5	1096964		Intergenic	10
5	1192574		Intergenic	16
6	689064		Intergenic	22
7	1288847	MAL7P1.164 (adapter-related protein)	Intron	10
8	368364		Intergenic	19
8	385626	MAL8P1.300 (conserved protein)	Intron	20
8	458876		Intergenic	13
8	632603		Intergenic	21
8	754504	MAL8P1.80 (conserved protein)	Intron	16
9	949883		Intergenic	4
11	1869584		Intergenic	21
12	529831	PFL0590c (PfATP4)	Nonsynonymous coding (cCa/cGa)	77
12	532193	PFL0590c (PfATP4)	Nonsynonymous coding (Ata/Cta)	76
12	2007366		Intergenic	20
13	1142115		Intergenic	23
13	2720098	PF13_0356 (conserved protein)	Intron	36
14	2264501		Intergenic	19
GNF-Pf4492R-3				
1	234556		Intergenic	23
3	76015		Intergenic	14
3	969681		Intergenic	13
5	134441		Intergenic	15
5	1096964		Intergenic	18
5	1192574		Intergenic	25
6	545594		Intergenic	34
6	1271683		Intergenic	8
8	458876		Intergenic	11
8	632603		Intergenic	24

		MAL8P1.80 (conserved		28
8	754504	protein)	Intron	
8	1011774		Intergenic	24
9	1404327		Intergenic	23
10	417810	PF10_0102 (ankyrin repeat)	Intron	41
		PF10_0366 (ADP/ATP	Nonsynonymous coding	36
10	1477944	transporter)	(aTt/aAt)	
11	354437		Intergenic	26
11	607299		Intergenic	26
11	1869584		Intergenic	28
			Nonsynonymous coding	93
12	532240	PFL0590c (PfATP4)	(gCt/gTt)	
13	1310242		Intergenic	24
13	2005305		Intergenic	19
14	389140		Intergenic	16
14	1895983		Intergenic	13
14	2088368		Intergenic	32

[a]Number of reads observed at that position for each SNV.

Table S3. PfATP4 SNVs identified in spiroindolone-resistant lines

Strain	Amino acid change
KAE609R-1	I398F, P990R, D1247Y
KAE609R-2	T418N, P990R
KAE609R-3	D1247Y
KAE678R-1	G223R
KAE678R-2	A184S, P990R
KAE678R-3	I203M, I263V

Table S4. Liver-stage activity of selected antimalarials.

Compound	IC_{50} (μM) ± SD
MFQ	>10 ± 0
ART	>10 ± 0
ATQ	.0038 ± 0.0009
GNF-Pf4492	>10 ± 0
KAF246	>10 ± 0
KAE609	>10 ± 0

Mean of 5 experiments in 4 replicates each. SD, standard deviation.

Table S5. Resting intracellular sodium concentrations

Strain	Mean ± SEM
$Dd2^{EF1}$	11.6 ± 0.354
GNF-Pf4492R-1	18.8 ± 2.83
GNF-Pf4492R-2	18.2 ± 0.0548
GNF-Pf4492R-3	9.7 ± 0.724

Mean of 5 experiments in 4 replicates each. SEM, standard error of the mean.

References

[1] Rottmann, M., McNamara, C., Yeung, B. K., Lee, M. C., Zou, B., Russell, B., Seitz, P., Plouffe, D. M., Dharia, N. V., Tan, J., Cohen, S. B., Spencer, K. R., Gonzalez-Paez, G. E., Lakshminarayana, S. B., Goh, A., Suwanarusk, R., Jegla, T., Schmitt, E. K., Beck, H. P., Brun, R., Nosten, F., Renia, L., Dartois, V., Keller, T. H., Fidock, D. A., Winzeler, E. A., and Diagana, T. T. (2010) Spiroindolones, a potent compound class for the treatment of malaria, *Science 329*, 1175-1180.

[2] Goodyer, I. D., and Taraschi, T. F. (1997) *Plasmodium falciparum*: a simple, rapid method for detecting parasite clones in microtiter plates, *Exp Parasitol 86*, 158-160.

[3] Plouffe, D., Brinker, A., McNamara, C., Henson, K., Kato, N., Kuhen, K., Nagle, A., Adrian, F., Matzen, J. T., Anderson, P., Nam, T. G., Gray, N. S., Chatterjee, A., Janes, J., Yan, S. F., Trager, R., Caldwell, J. S., Schultz, P. G., Zhou, Y., and Winzeler, E. A. (2008) *In silico* activity profiling reveals the mechanism of action of antimalarials discovered in a high-throughput screen, *Proc Natl Acad Sci U S A 105*, 9059-9064.

[4] Manary, M. J., Singhakul, S. S., Flannery, E. L., Bopp, S. E., Corey, V. C., Bright, A. T., McNamara, C. W., Walker, J. R., and Winzeler, E. A. (2014) Identification of pathogen genomic variants through an integrated pipeline, *BMC Bioinformatics 15*, 63.

[5] Cohen, S. B., Gaskins, C., and Nasoff, M. S. (2005) Generation of a monoclonal antibody agonist to toll-like receptor 4, *Hybridoma (Larchmt) 24*, 27-35.

[6] Kilpatrick, K. E., Wring, S. A., Walker, D. H., Macklin, M. D., Payne, J. A., Su, J. L., Champion, B. R., Caterson, B., and McIntyre, G. D. (1997) Rapid development of affinity matured monoclonal antibodies using RIMMS, *Hybridoma 16*, 381-389.

[7] Lambros, C., and Vanderberg, J. P. (1979) Synchronization of *Plasmodium falciparum* erythrocytic stages in culture, *J Parasitol 65*, 418-420.

[8] Meister, S., Plouffe, D. M., Kuhen, K. L., Bonamy, G. M., Wu, T., Barnes, S. W., Bopp, S. E., Borboa, R., Bright, A. T., Che, J., Cohen, S., Dharia, N. V., Gagaring, K., Gettayacamin, M., Gordon, P., Groessl, T., Kato, N., Lee, M. C., McNamara, C. W., Fidock, D. A., Nagle, A., Nam, T. G., Richmond, W., Roland, J., Rottmann, M., Zhou, B., Froissard, P., Glynne, R. J., Mazier, D., Sattabongkot, J., Schultz, P. G., Tuntland, T., Walker, J. R., Zhou, Y., Chatterjee, A., Diagana, T. T., and Winzeler, E. A. (2011) Imaging of *Plasmodium* liver stages to drive next-generation antimalarial drug discovery, *Science 334*, 1372-1377.

[9] Spillman, N. J., Allen, R. J., McNamara, C. W., Yeung, B. K., Winzeler, E. A., Diagana, T. T., and Kirk, K. (2013) Na(+) regulation in the malaria parasite *Plasmodium falciparum* involves the cation ATPase PfATP4 and is a target of the spiroindolone antimalarials, *Cell Host Microbe 13*, 227-237.

[10] Diarra, A., Sheldon, C., and Church, J. (2001) In situ calibration and [H+] sensitivity of the fluorescent Na+ indicator SBFI, *Am J Physiol Cell Physiol 280*, C1623-1633.